In-situ Synthesis of Oxide Dispersion Strengthened Alloy using Laser Powder-Directed Energy Deposition

Joowon Suh [a], Wonjong Jeong [b], Seungmun Jung [a], Young-Bum Chun [a], Heung Nam Han [c], Ho Jin Ryu [d], Hee-Suk Chung [e], Sang Sub Han [e], Suk Hoon Kang [a*]

[a]*Materials Safety Technology Development Division, Korea Atomic Energy Research Institute, Daejeon 34057, Republic of Korea*

[b]*Department of Industrial Laser Technology, Korea Institute of Machinery and Materials, Busan 46744, Republic of Korea*

[c]*Department of Materials Science and Engineering & Research Institute of Advanced Materials, Seoul National University, Seoul 08826, Republic of Korea*

[d]*Department of Nuclear and Quantum Engineering, Korea Advanced Institute of Science and Technology, Yuseong-gu, Daejeon 34141, Republic of Korea*

[e]*Electron Microscopy Group of Materials Science, Korea Basic Science Institute, Daejeon 34133, Republic of Korea*

[*]*Corresponding author: shkang77@kaeri.re.kr*

Keywords : ODS alloy, SANS, LP-DED, In-situ formation

1. Introduction

The oxide dispersion strengthened (ODS) alloys are time consuming to produce it using powder metallurgy (PM) process, so the additive manufacturing (AM) meets the requirement of time efficient and near net shape production of ODS alloy. Nevertheless, the mechanical properties of AM ODS alloy are lower than PM ODS alloy. To enhance the mechanical properties, the grain size and nano oxide dispersoid should be refined. Recently, the refined oxides are evolved during AM from melt pool in-situ oxidation [1-3]. During AM, the oxygen gas in reactive gas ($Ar+O_2$) is dissociated to oxygen atoms by laser interaction and form oxides when they meet the highly oxygen affinity elements such as Y or Ti. The objective of this study is to study the microstructure and oxide formation in ODS alloys using electron microscope, small angle neutron scattering (SANS).

2. Methods

The Fe-based ODS powder was sieved 53~150 μm and laser powder-directed energy deposited (LP-DED) with Insstek MX-400. The Fe, Cr, W, Y, Ti elements were added to crucible and thereafter gas atomization process was conducted. The oxygen was injected to melt pool using reactive gas ($Ar+O_2$). The LP-DED sample was electrical discharge machined and final polished until colloidal silica to remove residual stress. The grain size was measured by equivalent circle diameter from electron backscatter diffraction-inverse pole figure (EBSD-IPF) map. The nano oxides were observed by scanning transmission electron microscope (STEM). STEM sample was prepared by twin-jet electropolishing. The oxide size was measured and calculated by small angle neutron scattering (SANS) magnetic scattering obtained from KAERI HANARO 40M SANS [4]. The scatterings are lognormal fitted and the oxide radius and fraction are extracted from lognormal fitted results.

3. Results

3.1 Nano oxide observation

The Fig. 1 indicate the oxides distributed along solidification cell boundaries and the Fig. 2 represents the nano oxides distributed in α-Fe matrix. The white oxides in Fig. 2(a) are confirmed to $Y_2Ti_2O_7$ oxide by selected area diffraction pattern (SADP), which is general refined oxides in ODS alloys. The point energy dispersive X-ray spectroscopy (EDS) results in Table I shows that the oxides are Y, Ti, O rich. Initially, the Y and Ti are dissolved in ODS powder and during LP-DED, the $Y_2Ti_2O_7$ oxide formed because the Y and Ti are thermodynamically more stable to form oxide compared to Fe, Cr, and W [5].

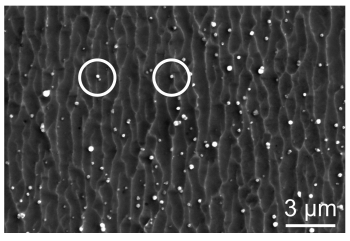

Fig. 1. (a) SEM image of ODS alloy.

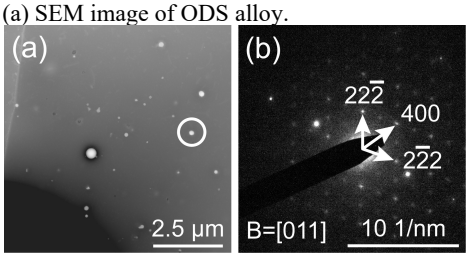

Fig. 2. (a) STEM image of ODS alloy, (b) SADP of white circle marked in (a).

Table I: Point EDS results of Fig. 2(a) white circle

Element	Fe	Cr	Y	Ti	O
Wt%	Bal.	6.6	26.8	18.4	4.9

3.2 Grain structure

The Fig. 3 shows the mixture of columnar and equiaxed grain structure of ODS alloys. The average grain size is 61.2 ± 28.7 μm, which is much finer than previous studies (>300 μm) [6]. The EBSD results indicate that the nano oxide effectively pin the grain growth during LP-DED. The oxide continuously suppress the movement of grain growth, resulting finer grain size and eventually they are distributed along solidification cell boundary, which is the end region of solidification process shown in Fig. 1.

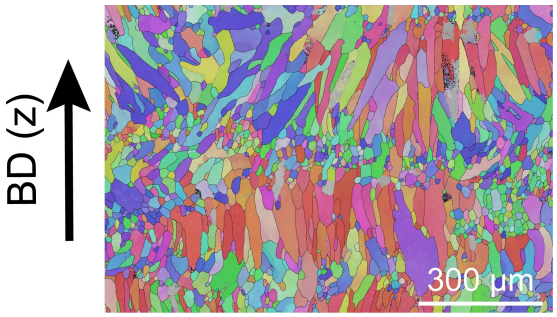

Fig. 3. EBSD IPF BD normal map

3.3 Measurement of oxide size, fraction from SANS

The oxide size, and fraction were calculated from lognormal fitted function in Fig. 4. The mean oxide size is 70.6 nm, and the volume fraction is 0.27%. The oxide size is much smaller than Y_2O_3 oxide coating powder used laser AM (L-AM) previous study [7] (mean oxide size 630 nm). First of all, the oxide was already coated on the powder surface in previous study and they could agglomerated during L-AM because the melting point of Y_2O_3 (2420 ºC) is higher than Fe (~1510 ºC). Compared to it, the nano oxide was in-situ formed during LP-DED in our study. As a result, the in-situ oxide agglomeration tendency is lower than already existing Y_2O_3. Secondly, the Y_2O_3 oxide refinement element, Ti was used in our study. $Y_2Ti_2O_7$ oxide is finer than Y2O3 because the coarsening kinetics of $Y_2Ti_2O_7$ is slower than Y_2O_3 [8].

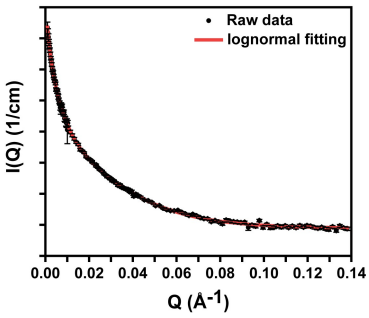

Fig. 4. SANS data of ODS alloy.

4. Conclusions

The microstructure and oxide were evaluated using SEM, STEM, EBSD, and SANS and the nano oxide refine the grain size. Thus, the in-situ oxidation is effective to evolve fine $Y_2Ti_2O_7$ oxide and thereafter these oxides suppress the movement of grain growth. This results show that the LP-DED in-situ oxidation is candidate process to fabricate fine nano oxide dispersed ODS alloy.

REFERENCES

[1] T. Horn, C. Rock, D. Kaoumi, I. Anderson, E. White, T. Prost, J. Darsell, Laser powder bed fusion additive manufacturing of oxide dispersion strengthened steel using gas atomized reaction synthesis powder, Materials & Design, 216, 110574, 2022.
[2] S. Saptarshi, M. DeJong, C. Rock, I. Anderson, R. Napolitano, J. Forrester, T. Horn, Laser Powder Bed Fusion of ODS 14YWT from Gas Atomization Reaction Synthesis Precursor Powders: Saptarshi, Dejong, Rock, Anderson, Napolitano, Forrester, Lapidus, Kaoumi, and Horn. *JOM*, *74*(9), 3303-3315, 2022.
[3] Austin, T. C., Sridharan, N., Massey, C., Lass, E. A., & Zinkle, S. Producing Oxide Dispersion Strengthened Fecral Using Directed Energy Deposition Additive Manufacturing with in Situ Oxidation. Available at SSRN 4503093.
[4] Y. S. Han, S. M. Choi, T. H. Kim, C. H. Lee, H. R. Kim, Design of 40M SANS instrument at HANARO, Korea. Physica B: Condensed Matter, 385, 1177-1179, 2006.
[5] J. Rieken, Gas atomized precursor alloy powder for oxide dispersion strengthened ferritic stainless steel (No. IS--T 3044). Ames Laboratory (AMES), Ames, IA (United States), 2011.
[6] Y. Shi, Z. Lu, L. Yu, R. Xie, Y. Ren, G. Yang, Microstructure and tensile properties of Zr-containing ODS-FeCrAl alloy fabricated by laser additive manufacturing. Materials Science and Engineering: A, 774, 138937, 2020.
[7] R. Streubel, M. B. Wilms, C. Doñate-Buendía, A. Weisheit, S. Barcikowski, J. H. Schleifenbaum, & B. Gökce, Depositing laser-generated nanoparticles on powders for additive manufacturing of oxide dispersed strengthened alloy parts via laser metal deposition. Japanese Journal of Applied Physics, 57(4), 040310, 2018.
[8] X. Boulnat, M. Perez, D. Fabrègue, S. Cazottes, Y. De Carlan, Characterization and modeling of oxides precipitation in ferritic steels during fast non-isothermal consolidation. Acta Materialia, 107, 390-403, 2016.